OMAE '99 Paper No: 99-6041 (Oral Presentation; not in Proceedings)

AIR GAP RESPONSE OF FLOATING STRUCTURES UNDER RANDOM WAVES: ANALYTICAL PREDICTIONS BASED ON LINEAR AND NONLINEAR DIFFRACTION

L. Manuel, S. R. Winterstein
Department of Civil Engineering
Stanford University, CA 94305-4020, USA

ABSTRACT

Two separate studies are presented here that deal with analytical predictions of the air gap for floating structures. (1) To obtain an understanding of the importance of first- and second-order incident and diffracted wave effects as well as to determine the influence of the structure's motions on the instantaneous air gap, statistics of the air gap response are studied under various modeling assumptions. For these detailed studies, a single field point is studied here – one at the geometric center (in plan) of the Troll semi-submersible.
(2) A comparison of the air gap at different locations is studied by examining response statistics at different field points for the semi-submersible. These include locations close to columns of the four-columned semi-submersible. Analytical predictions, including first- and second-order diffracted wave effects, are compared with wave tank measurements at several locations. In particular, the gross root-mean-square response and the 3-hour extreme response are compared.

BACKGROUND

The air gap response, and potential deck impact, of ocean structures under random waves is generally of considerable interest. While air gap modeling is of interest both for fixed and floating structures, it is particularly complicated in the case of floaters because of their large volume, and the resulting effects of wave diffraction and radiation. These give rise to two distinct effects: (1) global forces and resulting motions are significantly affected by diffraction effects; and (2) local wave elevation modeling can also be considerably influenced by diffraction, particularly at locations underneath the deck and/or near a major column. Both effects are important in air gap prediction: we need to know how high the wave rise (step 2), and how low the deck translates vertically (due to net heave and pitch) at a given point to meet the waves. Moreover, effects (1) and (2) are correlated in time, as they result from the same underlying incident wave excitation process.

We focus here on analytical diffraction models of air gap response, and its resulting stochastic nature and numerical predictions under random wave excitation. Attention is focused on a semi-submersible platform, for which both slow-drift motions (heave/pitch) and diffraction effects are potentially significant. Results are shown both from frequency-domain (including second-order transfer functions) and time-domain analyses. These permit careful study and isolation of various effects: e.g., wave forces on a fixed (locked-down) structure, the effect of structural motions on air gap response, and finally, the effect of different local wave elevation models in step 2. For reference, a complete second-order diffraction model is formulated and studied. Compared with this, various simplified models are imposed and evaluated: (a) second-order forces are estimated from mean drift forces only; and (b) second-order wave elevation effects are neglected completely, or these second-order effects are approximated by analytical Stokes theory, which retains second-order effects on the incident wave but neglects second-order diffraction. Use of (a) and (b) would significantly simplify the analysis, avoiding the costly step of second-order diffraction. While (a) is shown to be generally reliable, the local wave modeling in step (b) is found rather more sensitive to these precise modeling assumptions.

THEORY

Volterra Series and Transfer Functions

In modeling nonlinear systems, such as floating structures, it is common to employ Volterra series that permit one to describe the response (output) of such systems. The nonlinear system is defined in terms of first- and second-order transfer functions. For floating structures, these transfer functions are obtained from first- and second-order wave diffraction analysis programs such as WAMIT (e.g., WAMIT, 1995).

In order to study the response of a floating structure to random seas, we start by defining an irregular sea surface elevation, $h(t)$, which may be represented as a sum of sinusoidal components at N distinct frequencies as follows:

$$\begin{aligned} h(t) &= \sum_{k=1}^{N} a_k \cos(w_k t + q_k) \\ &= \mathrm{Re} \sum_{k=1}^{N} A_k \exp(i w_k t); \\ \text{where } a_k &= \sqrt{2 S_? (w_k) \Delta w}; \quad A_k = a_k \exp(i q_k) \end{aligned} \tag{1}$$

in which $S_\eta(w)$ represents a wave spectrum.

Any response quantity, $x(t)$, may be described by a second-order Volterra series representation as follows:

$$x(t) = x_1(t) + x_2(t) = x_1(t) + x_{2-}(t) + x_{2+}(t) \tag{2}$$

where $x_1(t)$, $x_{2-}(t)$, and $x_{2+}(t)$ are the first-order, second-order difference-frequency and second-order sum-frequency contributions, respectively, to the response. We can write each of these three components in terms of transfer functions. Thus,

$$\begin{aligned} x_1(t) &= \mathrm{Re} \sum_{k=1}^{N} A_k H_k^{(1)} \exp(i w_k t) \\ x_{2-}(t) &= \mathrm{Re} \sum_{k=1}^{N} \sum_{l=1}^{N} A_k A_l^* H_{kl}^{(2-)} \exp[i(w_k - w_l)t] \\ x_{2+}(t) &= \mathrm{Re} \sum_{k=1}^{N} \sum_{l=1}^{N} A_k A_l H_{kl}^{(2+)} \exp[i(w_k + w_l)t] \end{aligned} \tag{3}$$

In Equation (3), the transfer functions can describe any quantity of interest such as wave loads, platform motions, forces, etc.

Response Moments and Extremes

In the reliability analysis of offshore structures, response quantities of interest include extremes and fatigue damage. Exact statistics of these quantities are not known even for linear Gaussian responses; much less, for second-order Volterra models such as we use here. Hence, we must approximate these quantities, using limited response statistics for the process given by Equations (2) and (3). We choose here to characterize the physical response model by its first four statistical moments (mean, standard deviation, skewness, and kurtosis). Using these moments, we will estimate response extremes.

In order to obtain moments of the response process given in Equations (2) and (3), it is convenient to rewrite $x(t)$ in terms of standard Gaussian processes, $u_j(t)$ that are mutually independent at a fixed time, t. Thus, we have:

$$\begin{aligned} x_1(t) &= \sum_{j=1}^{2N} c_j u_j(t) \\ x_2(t) &= \sum_{j=1}^{2N} l_j u_j^2(t) \end{aligned} \tag{4}$$

The coefficients c_j and l_j are obtained by solving the eigenvalue problem of an integral equation involving the transfer functions and input power spectral densities (see Kac and Seigert, 1947). Once these coefficients are estimated, we can easily compute the first four statistical moments of the response. Hereinafter, to represent the first four statistical moments, we will employ the mean (m_x), standard deviation (s_x), and the dimensionless coefficients of skewness (a_{3x}) and kurtosis (a_{4x}) defined below:

$$\begin{aligned} m_x &= E[x(t)] \\ s_x^2 &= E[(x(t)-m_x)^2] \\ a_{3x} &= E[(x(t)-m_x)^3]/s_x^3 \\ a_{4x} &= E[(x(t)-m_x)^4]/s_x^4 \end{aligned} \tag{5}$$

In terms of c_j and l_j, the first four moments may be given as follows:

$$\begin{aligned} m_x &= \sum_{j=1}^{2N} l_j \\ s_x^2 &= \sum_{j=1}^{2N} (c_j^2 + l_j^2) \\ a_{3x} &= \frac{1}{s_x^3} \sum_{j=1}^{2N} (6c_j^2 l_j + 8l_j^3) \\ a_{4x} &= 3 + \frac{1}{s_x^4} \sum_{j=1}^{2N} (48c_j^2 l_j^2 + 48 l_j^4) \end{aligned} \tag{6}$$

Once these response moments are found, the response process *x(t)* may be related to a standard Gaussian process *u(t)* using a Hermite transformation model (Winterstein, 1988) as follows:

$$x = m_x + k s_x [u + c_3(u^2 - 1) + c_4(u^3 - 3u)] \tag{7}$$

where c_3, c_4 and κ are coefficients that can be estimated in terms of a_{3x} and a_{4x}.

The *p*-fractile extreme response in a seastate duration *T* can then be estimated from Equation (7) taking *u* as the corresponding Gaussian *p*-fractile extreme:

$$u_{\max,p} = [2\ln(\frac{n_0 T}{\ln(1/p)})]^{1/2} \tag{8}$$

where n_0 is the average response frequency.

Air Gap Response

In order to determine the instantaneous air gap, it is useful first to consider the net wave elevation, h_{NET}, with respect to a fixed origin. The logical next step is to consider the relative wave elevation *r(t)* measured with respect to the moving structure.

$$r(t) = h_{NET}(t) - d(t) \tag{9}$$

At the field point of interest, (*x*,*y*), *d(t)* denotes the net vertical displacement, which in turn is generally given in terms of the heave (x_3), roll (x_4), and pitch ((x_5), motions.

$$d(t) = x_3(t) + y \cdot x_4(t) - x \cdot x_5(t) \tag{10}$$

The available air gap *a(t)* is the difference between the still-water air gap and the relative wave, *r(t)*:

$$a(t) = a_0(t) - r(t) \tag{11}$$

The instantaneous net wave elevation, $h_{NET}(t)$, in Equation (9) is a result of both the incident waves that would occur if the structure were not present, and the diffracted waves that arise because of the presence of the structure that alters the flow field.

$$\begin{aligned} h_{NET}(t) &= h_{1,NET}(t) + h_{2,NET}(t) \\ h_{1,NET}(t) &= h_{1,I}(t) + h_{1,D}(t) \\ h_{2,NET}(t) &= h_{2,I}(t) + h_{2,D}(t) \end{aligned} \tag{12}$$

In Equation (12), we see that in our second-order model, we need to represent the net wave elevation as made up of first- and second-order waves; moreover, individually the incident waves (subscript: *I*) and the diffracted waves (subscript: *D*) will contribute to the first- and second-order waves. The first-order incident wave $h_{1,I}$ is modeled here as a stationary Gaussian process, and consistent values of $h_{1,D}$, $h_{2,I}$, and h_{2D} are calculated from hydrodynamic theory.

Application of Methodology to Floating Structures

The methodology using Volterra series models to describe the response of floating structures and the moment-based extreme estimation has been implemented in a post-processing analysis routine, TFPOP (Ude et al., 1996). This routine uses first- and second-order *force* transfer functions (from force calculations involving diffraction analysis) as well as added mass and damping (from first-order wave radiation). TFPOP combines these load transfer functions together with stiffness, damping, and inertia properties of the structure and, thus, constructs first- and second-order transfer functions to any response quantity, *x(t)*. In general, an analysis can include forces/moments in any of six degrees of freedom and can be used to estimate response quantities such as motions, accelerations, tether tensions, etc. The implementation and its theoretical basis (second-order model with moment-based extremes and fatigue estimation) have been verified in several previous studies. The different structures analyzed include TLP's, semi-submersibles, and spar buoys. Cases studied included TLP responses that were sensitive to second-order high-frequency loads (e.g., tether fatigue and heave acceleration – see Winterstein et al., 1994) as well as slow drift motions that were influenced by second-order low-frequency loads (e.g., surge motions of a TLP (Winterstein et al., 1994) and of a semi-submersible and a spar buoy (Winterstein et al., 1999)).

The air gap response introduced here presents several new and interesting challenges. It is the first response limit state where we need simultaneously include both second-order sum-frequency effects (on the wave surface), and second-order difference-frequency effects (on slow drift motions). The sum-frequency waves and the difference-frequency heave and pitch motions can both influence the air gap. The air gap response is further complicated because the heave, pitch, and roll motions of the floating structure are in general coupled. Moreover, the motions and the net wave elevation, both of which affect the air gap, are correlated in time as they result from the same underlying incident wave excitation process.

The air gap response, as described by Equations (9) through (12) above, has been implemented in the formulation based on second-order Volterra series and moment-based extremes models (Manuel and Winterstein, 1998). Options are available to selectively include or exclude the various contributions to the net wave elevation in Equation (12) – thus, one can study the relative influence of first- versus second-order waves, of incident versus diffracted waves, etc.

PLATFORM DESCRIPTION

The structure chosen for the numerical studies is the Troll semi-submersible. Figure 1 shows a plan view of the platform that has four columns and plan dimensions, 100 m^2 X 100 m^2. The still-water air gap is 25 meters and the mean water depth is 325 meters. Measurements of air gap were made at seven different field point locations. At

these same locations, WAMIT diffraction analyses were performed for waves with different headings and with wave periods ranging from 7.4 to 20.0 seconds. The seven field points locations are indicated on Figure 1.

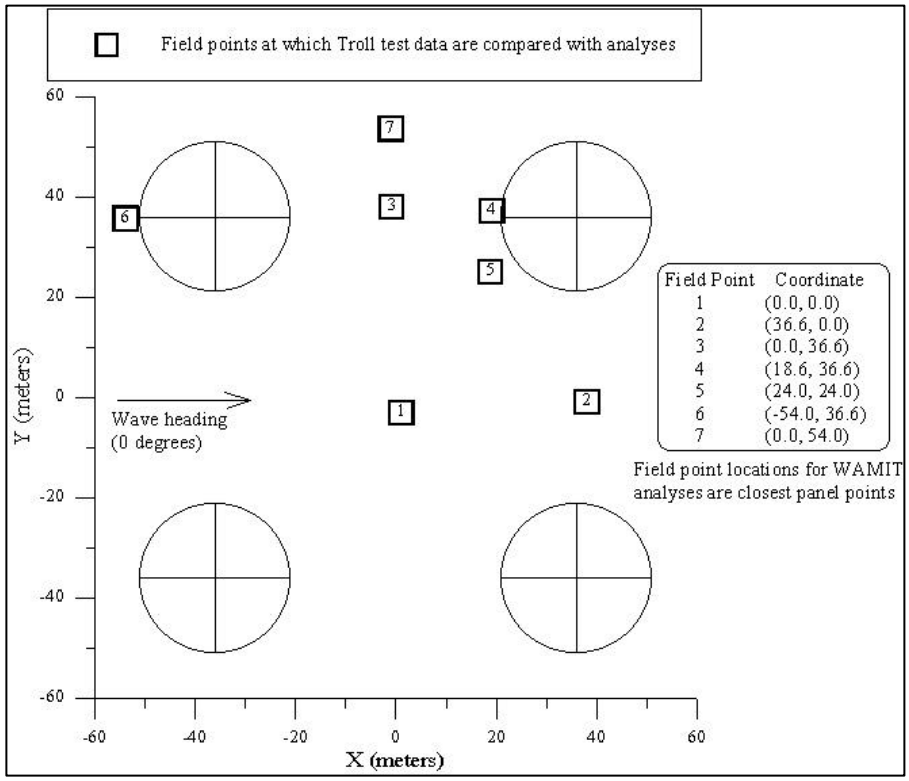

Figure 1. Plan view of Troll semi-submersible showing field points studied.

RESULTS I: PARAMETRIC STUDY AT MID-POINT LOCATION

We first consider analytical predictions of the relative wave elevation for the Troll semi-submersible. We are interested here in predicting the influence of alternative modeling options in describing the relative wave. For the sake of this exercise, we will study the air gap at a location directly below the center of the platform in plan. This is field point no. 1 in Figure 1. We consider a single seastate of 3 hours duration that is characterized by head seas (zero-degree heading) with a significant wave height of 10.6 meters and a spectral peak period of 12.5 seconds. This is a seastate for which model tests are available for comparison.

To isolate the effects of incident and diffracted waves of first- and second-order, and the effect of net vertical motion, we consider the following cases:

Case 0 Only first-order incident waves ($h_{1,I}$) included; structure locked down (i.e., motions prevented, $d = 0$)

Case 1 Only first- and second-order incident waves ($h_{1,I}$ and $h_{2,I}$) included; structure locked down

Case 2 First-order incident and diffracted waves ($h_{1,I}$ and $h_{1,D}$), second-order incident waves ($h_{2,I}$) included; structure locked down

Case 3 First- and second-order incident and diffracted waves ($h_{1,I}$, $h_{1,D}$, $h_{2,I}$, and $h_{2,D}$) included; structure locked down

Heave Structure's heave motion (x_3) studied.

Base First- and second-order incident and diffracted waves ($h_{1,I}$, $h_{1,D}$, $h_{2,I}$ and $h_{2,D}$) included; structure permitted to move (i.e., $d \neq 0$)

Table 1 summarizes the response statistics for the Troll submersible in each of the case defined. (Note that all results seek to model the air gap response except "Heave", which reflects only the vertical structural motion.)

Contributions to the response statistics from the first-order effects are shown in the table. Also shown are the response statistics for the total response (a sum of first- and second-order contributions).

Type of Run	Response	Mean (m)	Std. Dev (m)	Skewness	Kurtosis	Median Extreme (m)	Peak Factor
Case 0	TOTAL	0.00	2.65	0.00	3.00	10.08 (-10.08)	3.8
Case 1	1st-order	0.00	2.65	0.00	3.00	10.08 (-10.08)	
	TOTAL	0.00	2.70	0.20	3.06	11.17 (-8.91)	4.1
Case 2	1st-order	0.00	3.25	0.00	3.00	12.08 (-12.08)	
	TOTAL	0.00	3.27	0.09	3.04	12.11 (-11.05)	3.7
Case 3	1st-order	0.00	3.25	0.00	3.00	12.08 (-12.08)	
	TOTAL	0.00	3.50	0.54	4.12	19.23 (-12.54)	5.5
Heave	1st-order	0.00	0.78	0.00	3.00	2.81 (-2.81)	
	TOTAL	0.07	0.79	0.21	3.13	3.34 (-2.54)	4.1
Base	**1st-order**	**0.00**	**2.52**	**0.00**	**3.00**	**9.44 (-9.44)**	
	TOTAL	**-0.07**	**2.85**	**0.50**	**4.55**	**17.18 (-12.38)**	**6.1**

Table 1 Response Statistics for Cases involving different Modeling Options

From the table, the following findings may be noted as we move across the various cases:

Case 0 Because Case 0 includes only first-order incident waves, the net wave elevation (TOTAL) is seen to be Gaussian as expected. Also, the rms response (2.65 meters) is equal to one-fourth of the significant wave height (10.6 meters) as expected. The Gaussian character of the response is also confirmed by the peak factor on the median extreme of 3.8 (see Equation 3.8 with $p = 0.5$, $n_0T = 1080$) which would be expected for a seastate of duration, T equal to 3 hours.

Case 1 Case 1 includes a second-order Stokes incident wave process, which causes the net wave elevation to be non-Gaussian and positively skewed. The second-order process provides a small contribution to the total response: its rms is only 14 percent of that of the 1st-order process. The peak factor of the total process is 4.1 (only slightly non-Gaussian).

Case 2 Addition of the first-order diffracted waves in Case 2 (relative to Case 1) has the effect of raising the rms of the first-order process by 23% and the median extreme by 20%. (Because a linear effect has been added, we would expect roughly proportional increases in rms and extreme levels.) The peak factor of the total process response is 3.7 (i.e., the total process is more Gaussian than in Case 1 due to the larger relative contribution of the first-order effects).

Case 3 Addition of second-order diffracted waves in Case 3 (relative to Case 2) causes a large increase in response, most notably in its extreme levels. In particular, the rms level changes only from 3.27 to 3.50, while the peak factor grows from 3.7 to 5.5. As we shall see below, these larger peak factors may be more consistent with the observed behavior in model test experiments. Note also that these enhanced peak factors are due to the marked non-Gaussian behavior predicted in this case: the skewness value is predicted to be 0.54, and the kurtosis value to be 4.12.

Heave The results for heave motions again show that nonlinear effects (here, the effect of difference-frequency slow-drift motions) only mildly influence rms values (0.78 increases only to 0.79), but more notably increases skewed, non-Gaussian behavior (skewness value of 0.21).

Base Finally, the base case results predict the relative wave response, from a structure now permitted to move. These results combine our "best" model of the wave elevation (including second-order diffraction effects as in Case 3) with our correlated model of associated vertical motions (at this midpoint location, due to heave only). As in Case 3, the results here show particularly strong non-Gaussian behavior: skewness value of 0.54, kurtosis of 4.55, and peak factor of 6.1. In view of their similarity with Case 3 values, these strongly non-Gaussian effects appear due to the presence of second-order diffracted waves, and are not weakened when structural motions are included. Of course, by permitting the structure to move with the waves, the relative wave response is reduced as compared with the locked-down structure in Case 3: reductions in standard deviations from 3.50m to 2.85m, and in median extremes from 19.23m and 17.18m. These reductions appear quite consistent with the marginal heave statistics shown in Table 1.

RESULTS II: BEST PREDICTIONS VERSUS OBSERVATIONS AT SELECTED LOCATIONS

We next study three different field point locations and compare analytical predictions with model test results. Four different seastates are considered:

1. H_s = 10.6m, T_p = 12.5s
2. H_s = 12.6m, T_p = 13.5s
3. H_s = 13.3m, T_p = 13.0s
4. H_s = 14.5m, T_p = 14.0s

These four seastates are chosen to conform with 3-hour model tests, all performed for head seas. Results are shown below for three field points, including again the platform mid-point and two other locations nearer to columns. In all cases, we focus on numerical values of the rms and peak factor (PF) only.

We first compare results from two different models: the most detailed model (the earlier "base" case), and its nearest competitor (which neglects second-order diffraction effects on the wave elevation, calculated at each field point). Note that this second-order term is likely the most expensive quantity to calculate within the numerical, boundary-value diffraction analysis. It is also perhaps the quantity most subject to questions of adequate modeling, meshing, etc. As such it is interesting to consider whether the far less costly results that ignore second-order diffraction effects – but include second-order incident wave effects from Stokes theory – can serve as a useful approximation to the more expensive, base case results.

Field Point 1 (at center)

H_s (m)	T_p (s)	Analysis w/o 2nd-order diff. TF		Analysis w/ 2nd-order diff. TF		Wave Tank Tests	
		σ (m)	PF	σ (m)	PF	σ (m)	PF
10.6	12.5	2.55	3.7	2.85	6.0	-	-
12.6	13.5	2.96	3.8	3.37	6.2	2.78	6.5
13.3	13.0	3.19	3.8	3.71	6.4	-	-
14.5	14.0	3.34	3.8	3.89	6.4	3.20	4.3

Field Point 5 (on diagonal @ 24,24)

Hs (m)	Tp (s)	Analysis w/o 2nd-order diff. TF		Analysis w/ 2nd-order diff. TF		Wave Tank Tests	
		σ (m)	PF	σ (m)	PF	σ (m)	PF
10.6	12.5	3.16	4.1	3.26	5.3	-	-
12.6	13.5	3.53	4.1	3.68	5.6	3.56	4.6
13.3	13.0	3.87	4.2	4.05	5.7	-	-
14.5	14.0	3.93	4.2	4.15	5.8	4.10	5.1

Field Point 6 (in front of a column)

Hs (m)	Tp (s)	Analysis w/o 2nd-order diff. TF		Analysis w/ 2nd-order diff. TF		Wave Tank Tests	
		σ (m)	PF	σ (m)	PF	σ (m)	PF
10.6	12.5	3.62	3.7	3.66	3.7	-	-
12.6	13.5	3.78	3.7	3.85	4.1	2.69	6.3
13.3	13.0	4.29	3.7	4.37	4.0	-	-
14.5	14.0	4.13	3.8	4.24	4.4	3.17	5.7

Comparing the results of the two models (in Table 2), second-order diffraction is found to (1) only moderately increase the rms response, but (2) markedly increase peak factors and hence predicted extremes. Thus, even if second-order effects in the incident wave are retained, unconservative air gap predictions may result if second-order

diffraction effects are neglected. The strength of this second-order diffraction correction is found to depend on the location; particularly strong non-Gaussian behavior is predicted at the platform mid-point, as compared with predictions corresponding to other points nearer a column.

Finally, we compare the model predictions with the observed wave tank statistics, shown in the final two columns of Table 2. We first note that these observed extremes (peak factors) each arise from a single 3-hour test, and are therefore rather noisy estimates of the median values across many similar 3-hour conditions. Even with that caveat, these results strongly suggest that second-order diffraction effects should not be ignored. Models that ignore these effects underestimate the observed peak factors, across all tests and locations considered.

When second-order diffraction effects are included, peak factors are no longer systematically underestimated. Agreement with observations remains imperfect, however. At some locations such as the platform midpoint, the predictions may appear somewhat "too nonlinear." Nonetheless, these results suggest that nonlinear diffraction effects can be important, and should be studied further. We believe that the general statistical models presented here, which estimate extremes from a limited set of statistical moments, offer an efficient approach to assess the impact of various nonlinear models on extreme response levels.

CONCLUSIONS

We have presented a methodology for describing the net wave elevation and, hence, the air gap response for floating structures. The formulation has been demonstrated to allow different levels of modeling of the net wave elevation and the relative wave in describing the response of interest. For example, the second-order diffracted waves may be omitted from the analysis if only a first-order diffraction analysis was carried out.

The relative importance of the incident waves relative to the diffracted waves of both first- and second-order has been studied. We find that, for the Troll semi-submersible, a full second-order analysis (including incident and diffracted waves up to second order) is necessary; it is unconservative to neglect the second-order diffracted waves (something that is often necessary because second-order diffraction analyses can be expensive).

In comparing the different field point locations, we find important non-Gaussian effects that differ slightly depending on the field points' proximity to a column. A field point at the center of the platform exhibited the greatest non-Gaussian character relative to field points near a column. The non-Gaussian character is largely a result of second-order diffracted waves.

ACKNOWLEDGMENTS

The authors gratefully acknowledge the support provided by a grant from the Offshore Technology Research Center. Additional support was provided by the sponsors of Stanford University's Reliability of Marine Structures (RMS) program: ABS, Aker, Amoco, BP, Chevron, DNV, Exxon, Mobil, Norsk Hydro, Saga, Shell, Statoil, and Texaco.

REFERENCES

1. Kac, M. and A. J. F. Seigert (1947). "On the Theory of Noise in Radio Receivers with Square Law Detectors," Journal of Applied Physics, Vol. 18, pp. 383-400.
2. Manuel, L. and S. R. Winterstein (1998). "Estimation of Air Gap Statistics for Floating Structures: Release of TFPOP Version 2.2 – A Computer Program for Performing Stochastic Response Analysis of Floating Structures," Technical Note TN-4, Reliability of Marine Structures Program, Stanford University.
3. Ude, T. C., S. Kumar, and S. R. Winterstein (1996). "TFPOP 2.1: Stochastic Response Analysis of Floating Structures under Wind, Current, and Second-Order Wave Loads," Technical Report RMS-18, Reliability of Marine Structures Program, Stanford University.
4. WAMIT, 4.0 (1995). "WAMIT: A Radiation-Diffraction Panel Program for Wave-Body Interaction – Users' Manual," Dept. of Ocean Engineering, M.I.T.
5. Winterstein, S.R. (1988). "Nonlinear Vibration Models for Extremes and Fatigue," Journal of Engineering

Mechanics, ASCE, Vol. 114, No. 10, pp. 1772-1790.
6. Winterstein, S. R., T. C. Ude, and G. Kleiven (1994). "Springing and Slow-Drift Responses: Predicted Extremes and Fatigue vs. Simulation," Proceedings, BOSS-94, Vol. 3, Massachusetts Institute of Technology, pp. 1-15.
7. Winterstein, S. R., A. K. Jha, and S. Kumar (1999). "Reliability of Floating Structures: Extreme Response and Load Factor Design," Journal of Water, Port, Coastal and Ocean Engineering, ASCE, Vol. 125, No. 4.